Strange hadron matter and SU(3) symmetry

V. G. J. Stoks[1,2] and T.-S. H. Lee[1]

[1]*Physics Division, Argonne National Laboratory, Argonne, Illinois 60439*
[2]*Centre for the Subatomic Structure of Matter, University of Adelaide, SA 5005, Australia*

We calculate saturation curves for strange hadron matter using recently constructed baryon-baryon potentials which are constrained by SU(3) symmetry. All possible interaction channels within the baryon octet (consisting of $N, \Lambda, \Sigma,$ and Ξ) are considered. It is found that a small Λ fraction in nuclear matter slightly increases binding, but that larger fractions ($>10\%$) rapidly cause a decrease. Charge-neutral $\{N, \Lambda, \Xi\}$ systems, with equal densities for nucleons and cascades, are only very weakly bound. The dependence of the binding energies on the strangeness per baryon, f_s, is predicted for various $\{N, \Lambda, \Xi\}$ and $\{N, \Lambda, \Sigma, \Xi\}$ systems. The implications of our results in relativistic heavy-ion collisions and the core of a dense star are discussed. We also discuss the differences between our results and previous hadron matter calculations. [S0556-2813(99)06108-7]

I. INTRODUCTION

The study of the properties of strangeness-rich systems is of fundamental importance in understanding relativistic heavy-ion collisions [1] and some astrophysical problems [2]. The qualitative features of such systems and their possible detection in the universe and in relativistic heavy-ion collisions were first discussed by Bodmer [3] in 1971. Within quantum chromodynamics (QCD), it was suggested that the strangeness-rich systems could be strange quark systems consisting of up (u), down (d), and strange (s) quarks. These exotic systems could be either metastable states [4] against the decays into hadrons, or absolute bound states with energies much lower than normal nuclear matter [5,6]. However, the theoretical calculations for strange quark systems are still in the developing stage. For example, within the MIT bag model it is found [7] that the stability of the bag strongly depends on the rather uncertain bag constant B_{bag}. The strange quark matter is absolutely stable for $B_{bag}^{1/4}$ ~ 140 MeV, metastable for $B_{bag}^{1/4} = 150-200$ MeV, and unstable for $B_{bag}^{1/4} > 200$ MeV. Therefore, one cannot rule out the possibility that the strangeness-rich systems could be strange hadron systems made of nucleons and hyperons; as studied, for example, in Refs. [8–12].

The production and detection of strangeness-rich matter from relativistic heavy-ion collisions has been studied in recent years [13–17,7]. Two scenarios have been discussed. The first one is the coalescent mechanism [17], which assumes that the produced hyperons are captured by the nearby nuclear fragments in the freeze-out region to form multihyperon clusters. The second mechanism is the distillation process [13–15,7] associated with the production of a quark-gluon plasma (QGP) in the baryon-rich region. The essential idea is that the $\bar{s}$ quarks in a QGP, in which $s\bar{s}$ pairs are abundant, are captured by the surrounding u and d quarks, liberated from the initial heavy ions, to form K^+ and K^0. The emission of these kaons and other mesons causes cooling of the QGP into a strange quark system. The interesting question to ask is whether this system will be absolutely stable or

metastable against the collapse into a hadron system. This question can be answered by comparing the energy of such a system with the energy of a strange hadron system with the same strangeness quantum number. It is therefore important to develop theoretical approaches to calculate the energies of strange hadron systems. In this paper, we report on the first results of our efforts in this direction. The calculation for the strange quark systems with similar sophistication is beyond the scope of this paper.

Most of the recent investigations of strange hadron systems have been done by using the relativistic mean-field model [9–11,7]. In addition to the usual σ and ω mesons, these models also contain σ^* and ϕ mesons, introduced in order to have strong attractive hyperon-hyperon interactions. The vector coupling constants are chosen according to SU(6) symmetry, while the scalar coupling constants are fixed to hypernuclear data. Extensive calculations for the systems consisting of $\{p, n, \Lambda, \Xi^0, \Xi^-\}$ mixtures have been performed. Clearly, these calculations are not completely consistent with the SU(3) symmetry, since Σ's are not included (for reasons that will be discussed below). Furthermore, it is not clear that the values for the coupling constants employed in these models are consistent with the very extensive data on nucleon-nucleon (NN) and hyperon-nucleon (YN) reactions. A rigorous prediction should be consistent with both the two-body data and the data of hypernuclei.

An alternative approach is based on the many-body theory with baryon-baryon potential models. This was first pursued by Pandharipande [8] using a variational method and rather crude baryon-baryon potentials. This approach has recently be revived in Ref. [12] by using the Brueckner-Hartree-Fock approximation and the Nijmegen soft-core YN potential [18] of 1989. There, the authors only consider an infinite system consisting of Λ's and nucleons. It was found that for a given total baryon density ρ_B the binding energy per baryon, $E_B = -E/A_B$, decreases as the fraction of strangeness, $f_s = |S/A_B|$, increases. The most stable system in their approach has $E_B = -E/A_B \sim 16.0$ MeV, at $f_s \sim 0.06$ and $\rho \sim 0.23$ fm^{-3}. Comparing with the calculations using relativistic mean-field models as described above, this investigation

is rather incomplete since the role of Ξ is not explored, owing to the restriction of the employed Nijmegen potential. The importance of Ξ was pointed out in Ref. [9]. It is needed to stabilize the system against the strong $\Lambda + \Lambda \rightarrow \Xi + N$ process, which can occur at relatively low density of Λ since the threshold energy for this reaction to occur is only about 28 MeV. The presence of Ξ will Pauli block this reaction. Furthermore, their calculations do not include hyperon-hyperon interactions and hence the effects of additional hyperons on the hyperon mean field are neglected in solving the self-consistent G-matrix equation. In this paper we try to be as complete as possible in that we include all possible interaction channels that are allowed for the baryon octet. We use the recently constructed NSC97 baryon-baryon potential models [19,20] to describe all these channels.

The content of the paper is as follows. In Sec. II we briefly highlight some of the features of the employed baryon-baryon potential models. In Sec. III we review the definition of the G matrix and related quantities, with some emphasis on the treatment of the coupled channels. In Sec. IV we present and discuss the results of our calculations. We conclude with a brief summary of our findings in Sec. V.

II. BARYON-BARYON POTENTIAL

In this paper, we report on the first results from an investigation of strange hadron matter using the most recently developed baryon-baryon potentials [19,20]. These potentials are constructed within the dynamics defined by the SU(3) symmetry, and the data of nucleon-nucleon (NN) and hyperon-nucleon (YN) reactions. We follow a similar Brueckner-Hartree-Fock formulation as recently employed by Schulze *et al.* [12], but with an important improvement: the starting coupled-channel $NN \oplus YN \oplus YY$ potentials include the $\Lambda\Lambda, \Lambda\Sigma, \Sigma\Sigma$, and ΞN channels of strangeness $S = -2$, as required by SU(3) symmetry. The presence of Ξ then also enforces us to consider the $\Xi\Lambda$ and $\Xi\Sigma$ channels of strangeness $S = -3$, and the $\Xi\Xi$ channel of strangeness $S = -4$. The assumption of SU(3) symmetry allows us to unambiguously define the baryon-baryon interactions for the $S = -2, -3, -4$ systems from the previously constructed NN and YN interactions.

However, because of the lack of sufficiently accurate YN data and some uncertainties in SU(3) coupling constants, the constructed baryon-baryon potentials have some model dependence. In Ref. [19], six YN models have been constructed, based on different choices for the vector-magnetic $F/(F+D)$ ratio, α_V^m. Values range from $\alpha_V^m = 0.4447$ for model NSC97a to $\alpha_V^m = 0.3647$ for model NSC97f. The different choices for α_V^m (consistent with static or relativistic SU(6) predictions) are chosen such that the models encompass a range of scattering lengths in the ΣN and ΛN channels, but all models describe the YN scattering data equally well. Differences show up in more elaborate applications such as hypernuclear calculations; see Ref. [19] for a more detailed discussion. In this paper we will only consider models NSC97e and NSC97f, which seem to be the most consistent with the existing hypernuclear data [19].

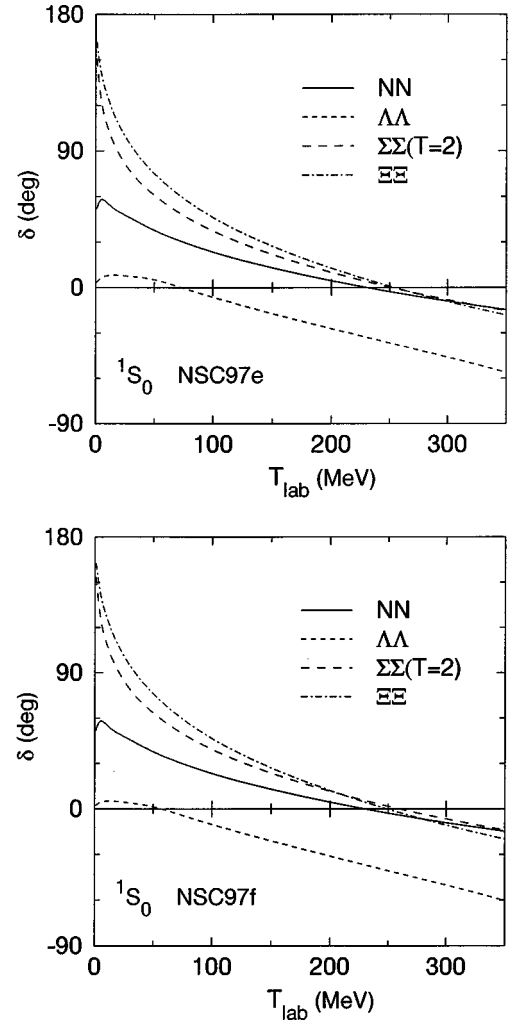Another important assumption in the construction of the

FIG. 1. $^1S_0$ phase shifts for elastic identical-particle scattering, for models NSC97e and NSC97f.

baryon-baryon potentials is that the SU(3) symmetry is applied to the full range of the interaction; i.e., to the long-range as well as to the short-range part. Although there is no empirical evidence that the short-range part indeed satisfies the SU(3) symmetry (there are no YY scattering data to test this assumption, for example, with these potential models), we have chosen for this approach since it allows us to extend the NN and YN interactions to all YY interactions describing the $S = -2, -3, -4$ systems, without having to introduce any new parameters. To illustrate the differences between the various interactions, we show in Fig. 1 the $^1S_0$ elastic phase shifts for the two models in the $NN, \Lambda\Lambda, \Sigma\Sigma(T=2)$, and $\Xi\Xi$ channels. The differences between NSC97e and NSC97f are fairly small and, at this scale, will only show up in the $\Lambda\Lambda$ channel. A more detailed description of the NSC97 potential models in the YY channels is presented elsewhere [20].

III. G-MATRIX FOR COUPLED CHANNELS

In the next section we will present the results of several Brueckner-Hartree-Fock calculations using the baryon-

baryon potentials for the $S=0,\ldots,-4$ systems, and so here we review some of the aspects of the G matrix and define the relevant quantities. In each case, the (strange) nuclear matter is characterized by a total density ρ, which is broken up into the contributions from the four baryon species according to

$$\rho = \rho_N + \rho_\Lambda + \rho_\Sigma + \rho_\Xi$$

$$= \rho(\chi_N + \chi_\Lambda + \chi_\Sigma + \chi_\Xi)$$

$$= \frac{1}{3\pi^2}(2k_F^{(N)3} + k_F^{(\Lambda)3} + 3k_F^{(\Sigma)3} + 2k_F^{(\Xi)3}). \tag{1}$$

This also defines the Fermi momentum $k_F^{(B)}$ for a baryon B with density fraction χ_B. As standard, we define the G matrix $G(\mathbf{p}_1',\mathbf{p}_2';\mathbf{p}_1,\mathbf{p}_2)$ for incoming (unprimed) and outgoing (primed) momenta. Defining mass fractions $\mu_i = M_i/(M_1+M_2)$, the total momentum is $\mathbf{P} = \mathbf{p}_1 + \mathbf{p}_2 = \mathbf{p}_1' + \mathbf{p}_2'$, and the relative momenta are given by $\mathbf{k} = \mu_2\mathbf{p}_1 - \mu_1\mathbf{p}_2$ and $\mathbf{k}' = \mu_2\mathbf{p}_1' - \mu_1\mathbf{p}_2'$. The G matrix satisfies the Bethe-Goldstone equation [21]

$$G(\mathbf{k}',\mathbf{k};\mathbf{P},\omega) = V(\mathbf{k}',\mathbf{k}) + \int \frac{d^3q}{(2\pi)^3} V(\mathbf{k}',\mathbf{q})$$

$$\times \frac{Q(\mathbf{q},\mathbf{P})}{\omega - E_1(\mu_1\mathbf{P}+\mathbf{q}) - E_2(\mu_2\mathbf{P}-\mathbf{q})}$$

$$\times G(\mathbf{q},\mathbf{k};\mathbf{P},\omega), \tag{2}$$

where $Q(\mathbf{q},\mathbf{P})$ is the Pauli operator which ensures that the intermediate-state momenta are above the Fermi sea (see below). The ω denotes the starting energy (including rest masses), while the intermediate-state energies are given by

$$E_1(\mathbf{p}_1'') + E_2(\mathbf{p}_2'') = M_1 + M_2 + \frac{p_1''^2}{2M_1} + \frac{p_2''^2}{2M_2} + \mathrm{Re}\,U(\mathbf{p}_1'')$$

$$+ \mathrm{Re}\,U(\mathbf{p}_2'')$$

$$= M + \frac{P^2}{2M} + \frac{q^2}{2\mu} + \mathrm{Re}\,U(\mu_1\mathbf{P}+\mathbf{q})$$

$$+ \mathrm{Re}\,U(\mu_2\mathbf{P}-\mathbf{q}), \tag{3}$$

with M and μ the total and reduced mass, respectively. The single-particle potentials U are defined by

$$U(\mathbf{p}_1) = \int^{(k_F^{(B)})} \frac{d^3p_2}{(2\pi)^3} G[\mathbf{p}_1,\mathbf{p}_2;\mathbf{p}_1,\mathbf{p}_2;\omega = E_1(\mathbf{p}_1)$$

$$+ E_2(\mathbf{p}_2)], \tag{4}$$

where it is to be understood that the Fermi momentum $k_F^{(B)}$ is associated with the particle which has momentum p_2. Hence, we have two equations, Eqs. (2) and (4), which have to be solved self-consistently.

In our calculations we have made several approximations. First of all, the energies are treated in the nonrelativistic

expansion, as is obvious from the $1/M^2$ expansion in Eq. (3). The same $1/M^2$ expansion was used in the derivation of the NSC97 potentials [19]. Brockmann and Machleidt [22] have demonstrated the effect on nuclear-matter results when one uses instead the relativistic energies and the Dirac equation for the single-particle motion; these type of calculations have become known as Dirac-Brueckner calculations. For purely nuclear matter they find that the saturation point shifts to lower density and has a smaller binding energy per nucleon. In analogy with their result, we expect that a proper Dirac-Brueckner calculation for strange nuclear matter will also show a shift of saturation points as compared to what we find in our present Brueckner-Hartree-Fock calculations. However, we believe that the calculations presented here suffice for our purpose, which is to study the general features of strange nuclear matter. Any shift of saturation points is only expected to be relevant in those cases where the matter under consideration is on the boundary of being bound or unbound. In those cases, the Dirac-Brueckner result might show that matter which we find to be just bound is actually unbound, or vice versa.

A second approximation is that the single-particle potential is radically put to zero for momenta $\mathbf{p}_i$ above the Fermi sea: the so-called ''standard'' choice. This causes a discontinuous jump in $E_i(p_i)$ at $p_i = p_F$, and so it is also known as the ''gap'' choice. An alternative choice is to retain a nonzero value for momenta above the Fermi sea: the so-called ''continuous'' choice [23]. There are various physical arguments which favor this latter choice [23], but its main effect is to merely shift the saturation curve to give more binding, without changing the overall density dependence very much; see, e.g., Refs. [24,25] for the effect in ordinary nuclear matter. However, these differences are only of relevance on a quantitative level (e.g., when a comparison is made with the experimental saturation point), and so we argue that for this first study of the general features of strange nuclear matter it suffices to use the gap choice. Another motivation is that the continuous choice considerably complicates the propagator in the Bethe-Goldstone equation, which makes the calculations much more cumbersome and computer intensive.

A further simplification in the self-consistency calculation is that we assume a quadratic momentum dependence for the single-particle potential $U(p)$. This means that we can define an effective baryon mass M^* in terms of which the single-particle energy can be written as

$$E_i(p) = M_i + \frac{p^2}{2M_i} + \mathrm{Re}\,U_i(p) \tag{5a}$$

$$\approx M_i + \frac{p^2}{2M_i^*} + \mathrm{Re}\,U_i(0), \tag{5b}$$

where $U_i(0)$ is easily obtained from Eq. (4), while M_i^* is obtained from

$$\frac{M_i^*}{M_i} = \left[1 + \frac{\mathrm{Re}\,U_i(p_F) - \mathrm{Re}\,U_i(0)}{p_F^2/2M_i}\right]^{-1}. \tag{6}$$

The advantage of using Eq. (5b) is that the self-consistency condition only needs to be calculated at $p=0$ and $p=p_F$, rather than at a range of momentum values $0 \leq p \leq p_F$, as required when using Eq. (5a). Also, the binding energy does not require a numerical integration, but is easily done analytically. We checked for various cases that the parametrization of Eq. (5b) indeed fairly accurately represents the single-particle energy as obtained from an explicit calculation using Eq. (5a).

In Eq. (2), the Pauli operator needs to be expressed in terms of **P** and **q**. Clearly, $|\mu_1 \mathbf{P}+\mathbf{q}| \geq k_F^{(1)}$ and $|\mu_2 \mathbf{P}-\mathbf{q}| \geq k_F^{(2)}$ are both satisfied when $q \geq \mu_1 P + k_F^{(1)}$ and $q \geq \mu_2 P + k_F^{(2)}$. Similarly, when $q^2 < k_F^{(1)2} - (\mu_1 P)^2$ or $q^2 < k_F^{(2)2} - (\mu_2 P)^2$ at least one of the inequalities is not satisfied. For values of q between these two limits, there are two restrictions on the angle $\theta(\mathbf{P},\mathbf{q})$, namely

$$\cos \theta > -\cos \theta_1 \equiv -\frac{(\mu_1 P)^2 + q^2 - k_F^{(1)2}}{2\mu_1 P q},$$

$$\cos \theta < \cos \theta_2 \equiv \frac{(\mu_2 P)^2 + q^2 - k_F^{(2)2}}{2\mu_2 P q}. \tag{7}$$

Since the angle $\theta(\mathbf{P},\mathbf{q})$ is integrated over, we can approximate this latter constraint by taking an average value for the Pauli operator Q. We therefore define

$$Q(q,P) = 1, \quad \text{if} \quad q \geq \max[\mu_1 P + k_F^{(1)}, \mu_2 P + k_F^{(2)}]$$

$$= 0, \quad \text{if} \quad q^2 < \max[k_F^{(1)2} - (\mu_1 P)^2, k_F^{(2)2} - (\mu_2 P)^2]$$

$$= \min[\cos \theta_1, \cos \theta_2], \quad \text{otherwise}. \tag{8}$$

In the partial-wave projection, the Bethe-Goldstone equation for a system with isospin T and total angular momentum J becomes

$$G_{l's',ls}^{JT}(q',q;P,\omega) = V_{l's',ls}^{JT}(q',q)$$

$$+ \frac{2}{\pi} \sum_{l''s''} \int dq'' q''^2 V_{l's',l''s''}^{JT}(q',q'')$$

$$\times \frac{Q(q'',P)}{\omega - M - P^2/2M - q''^2/2\mu - X + i\varepsilon}$$

$$\times G_{l''s'',ls}^{JT}(q'',q;P,\omega), \tag{9}$$

where $X=0$ for the gap choice and $X=U(|\mu_1 \mathbf{P}+\mathbf{q}|) + U(|\mu_2 \mathbf{P}-\mathbf{q}|)$ plus angle-averaging for the continuous choice. The single-particle potential is obtained self-consistently from

$$U(\mathbf{p}_1) = \sum_{T,J,l,s} \frac{(2J+1)(2T+1)}{(2s_1+1)(2t_1+1)} 2\pi$$

$$\times \int_{-1}^{+1} d\cos\theta \int_0^{k_F^{(B)}} \frac{p_2^2 dp_2}{(2\pi)^3} 4\pi G_{ls,ls}^{JT}$$

$$\times [k,k;P,E_1(p_1) + E_2(p_2)]_{AS}, \tag{10}$$

where we have explicitly separated off the angle dependence of the d^3p_2 integral. The isospin factors are present to account for all the contributions of the possible isospin states. (Our calculations are done on the isospin basis.) Finally, the subscript AS denotes that we have to include both direct and exchanged (Hartree and Fock) contributions. For identical particles, this can be accounted for by multiplying the G matrix from the Bethe-Goldstone equation with the factor $1 - (-1)^{l+s+\bar{t}}$, with $\bar{t}=1$ for singlet-even and triplet-odd partial waves and $\bar{t}=0$ for singlet-odd and triplet-even partial waves. (Note that $\bar{t}$ is equivalent to the isospin in the case of pure NN or pure $\Xi\Xi$ systems.)

If we now want to include all species of the octet baryons, the above expressions can be easily generalized. First, the internal sum over l'',s'' in the Bethe-Goldstone equation then also involves a sum over all possible channels allowed for a particular two-baryon interaction. Of course, the propagator needs to be modified to account for the relevant masses and thresholds in each particular channel, and the Pauli operator should contain the Fermi momenta belonging to the relevant species. Second, the single-particle potentials have to be summed over all baryon species. Using the notation $U_B^{(B')}$ for the single-particle potential of particle B due to the interactions with particles B' in the medium, and a bra-ket notation for the final-initial state particles, we have

$$U_B(\mathbf{p}_1) = \sum_{B'} U_B^{(B')}(\mathbf{p}_1), \tag{11}$$

where

$$U_B^{(B')}(\mathbf{p}_1) = \sum_{T,J,l,s} \frac{(2J+1)(2T+1)}{(2s_B+1)(2t_B+1)} 2\pi$$

$$\times \int_{-1}^{+1} d\cos\theta \int^{k_F^{(B')}} \frac{p_2^2 dp_2}{(2\pi)^3}$$

$$\times 4\pi \langle BB' | G_{ls,ls}^{JT}[k,k;P,E_1^{(B)}(p_1)$$

$$+ E_2^{(B')}(p_2)]_{AS} | BB' \rangle. \tag{12}$$

The allowed values of T,J,l,s depend on what particular baryons make up the scattering process $B + B' \rightarrow B + B'$. For example, $U_\Sigma^{(N)}$ gets contributions from direct isospin-3/2 ΣN scattering, but also from the coupled-channel isospin-1/2 $(\Lambda N, \Sigma N)$ scattering. In our calculations we include all partial waves up to $J=4$. Finally, the binding energy per baryon is obtained from

$$\frac{E}{A} \rho = \sum_B (2s_B+1)(2t_B+1) \int^{(k_F^{(B)})} \frac{d^3k}{(2\pi)^3} \left[\frac{k^2}{2M_B} + \frac{1}{2} U_B(k) \right]$$

$$= \frac{1}{2} \sum_B \rho_B \left[\text{Re } U_B(0) + \frac{3}{10} \left(\frac{1}{M_B^*} + \frac{1}{M_B} \right) k_F^{(B)2} \right]. \tag{13}$$
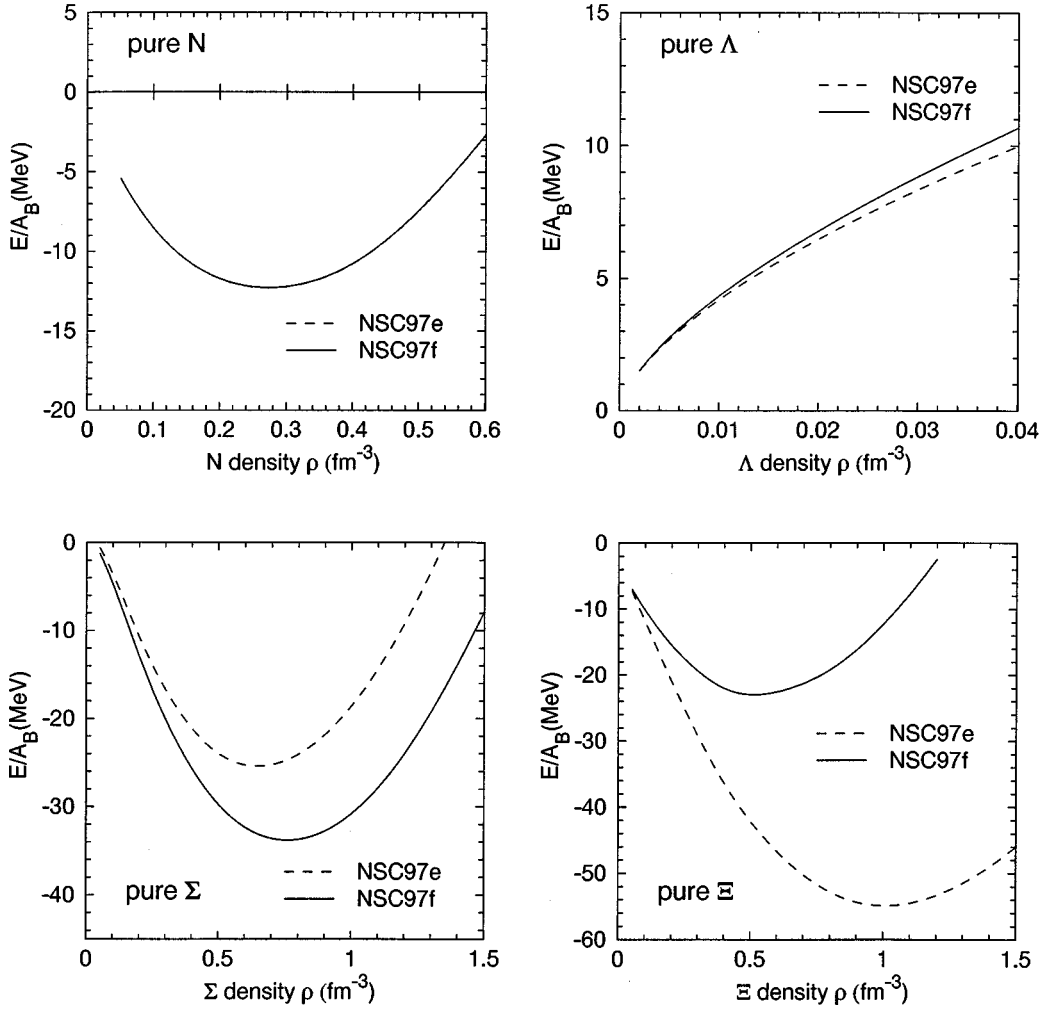
FIG. 2. Saturation of pure systems. The dashed curve and solid curve are the predictions of models (e) and (f), respectively. The pure Σ system represents the $T_z = \pm 2$ case without the Coulomb interaction. The results for the two NSC97 models for purely nuclear matter are practically indistinguishable and only the solid line is figured.

IV. RESULTS

A. Pure systems

The first interesting question to ask is whether all of the isospin symmetric matter ($T_z = 0$) made of only one kind of hadrons is bound. Our results are displayed in Fig. 2 for models NSC97e (dashed curves) and NSC97f (solid curves).

The saturation curves for the purely nuclear system are very similar to what is obtained for other one-boson-exchange NN potentials found in the literature. The results for the two NSC97 models are practically indistinguishable, which, in fact, is true for all six NSC97 models. This is a reflection of the fact that these models all describe the NN scattering data equally well.

We see that the pure Λ system is not bound at all for both models. The pure Λ system was calculated including the coupling to the ΞN and $\Sigma\Sigma$ channels. If this coupling is switched off (and so only elastic $\Lambda\Lambda$ scattering is possible), the curves shift to slightly higher values: about 10% higher for NSC97e and about 5% higher for NSC97f.

The pure Ξ system is more bound and saturates at higher densities than the nucleon system. The difference in the re-

sults for NSC97e and NSC97f is due to the fact that the $^3S_1$ partial-wave contribution to the single-particle potential (which is large and positive) for NSC97f is almost 40% larger than for NSC97e. In addition, the $^3P_2$ partial-wave contribution (which is also large, but negative) for NSC97f is about 10% less attractive and largely compensates for an increased attraction in the $^1S_0$ partial-wave contribution. An important part of the attraction is due to the scalar-exchange part of the potential. Since the existence of a nonet of scalar mesons with masses below 1 GeV/c is still highly controversial (especially the low-mass isoscalar σ meson), a comment is in order. We first note that within a one-boson-exchange model for the NN interaction, the scalar-exchange contribution plays a crucial role in providing the required attraction. Whether this contribution represents a true exchange of scalar mesons or just an effective parameterization of two-pion exchange and more complicated interactions is a question which goes beyond the scope of this paper. Here we only want to mention that arbitrarily removing the σ (or, in our case [19], the broad ε) contribution renders purely nuclear matter unbound at all densities. However, the pure Ξ

system still remains bound, although it saturates at a smaller density.

Pure Σ matter with $T_z=0$ is expected to be highly unstable, because it can decay strongly into Λ matter via $\Sigma^+\Sigma^-\to\Lambda\Lambda$ and $\Sigma^0\Sigma^0\to\Lambda\Lambda$. However, we can consider pure Σ^+ or pure Σ^- matter with $T_z=\pm2$, respectively. Inclusion of the Coulomb interaction in this charged system is beyond our present calculation (and is likely to modify the result), and so the third panel of Fig. 2 represents the result without the Coulomb interaction and is included for illustrative purposes only. The difference in the results for NSC97e and NSC97f is due to the fact that the single-particle potential for NSC97f is slightly more attractive for almost all partial-wave contributions, which adds up to a substantial difference in the total single-particle potential.

The results of these calculations show that for the employed baryon-baryon models of Refs. [19,20] the only possible long-lived strange pure system within SU(3) is the Ξ system, which is stable against strong decays. This suggests that the inner core of high-density astrophysical objects could be rich in Ξ particles, but to further investigate this requires much more elaborate calculations.

B. $\{N,\Lambda\}$ systems

We next consider the change of the nuclear binding by adding Λ's. The results are shown in Fig. 3. We should point out that, even though the Σ and Ξ are not explicitly included as part of the medium, the coupling to these particles via the transition potentials $V(\Lambda N\to\Sigma N)$ and $V(\Lambda\Lambda\to\Xi N,\Sigma\Sigma)$ *are* included. We see that the binding first slightly increases until the Λ fraction reaches about 10%. The system rapidly becomes less bound when more Λ particles are added.

The most stable system occurs at about $\rho=0.28$ fm^{-3} and $\chi_\Lambda=0.1$ with $E/A_B=-13.2$ MeV for NSC97e and at about $\rho=0.27$ fm^{-3} and $\chi_\Lambda=0.05$ with $E/A_B=-12.7$ MeV for NSC97f. The Λ fraction at the minimum is very similar to the $\chi_\Lambda\approx0.06$ found in Ref. [12], but in their case the minimum occurs at a lower density with a higher binding energy ($\rho=0.23$ fm^{-3} with $E/A_B=-16.0$ MeV). This difference is due to various reasons. First of all, the larger binding energy found in Ref. [12] is due to the fact that they use the continuous choice for the single-particle energy, whereas we use the gap choice. The smaller density at which their saturation occurs is due to the different NN potential that is employed: they use the parameterized Paris NN potential [26], whereas here we use the NN potential as given by the NSC97 models. Furthermore, the results of Ref. [12] do not include the effect of Λ's interacting with themselves. We *do* include the $\Lambda\Lambda$ interaction and, although we find that the contribution of $U_\Lambda^{(\Lambda)}$ to the total single-particle potential is rather small, its influence starts to become noticeable as the Λ density increases. At low Λ density the individual partial-wave contributions to $U_\Lambda^{(\Lambda)}$ are almost all negative, but as the Λ density increases some of them start to give (relatively important) positive contributions. As a consequence, the effect of the inclusion of the $\Lambda\Lambda$ interaction for increasing χ_Λ is to shift the density at which saturation occurs to lower values. The effect is most pronounced for
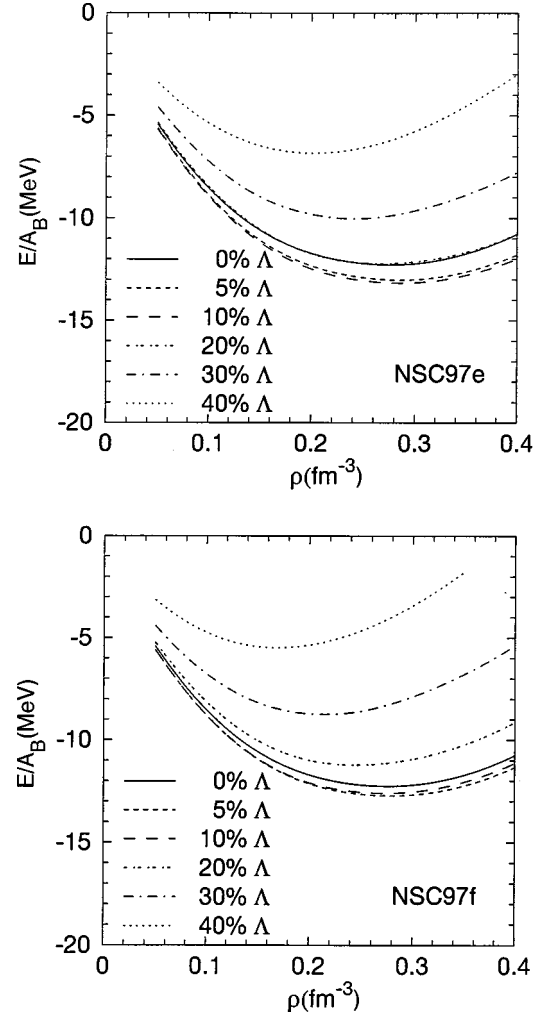

FIG. 3. Saturation of $\{N,\Lambda\}$ systems for various fractions $\rho_\Lambda/(\rho_N+\rho_\Lambda)$.

NSC97f. In Ref. [12] the saturation density is more or less independent of the Λ fraction; see their Fig. 5.

Our results suggest that multi-Λ systems produced in relativistic heavy-ion collisions through, for example, the coalescent mechanism could be loosely bound. However, the presence of a large fraction of Λ's in the inner core of a dense star seems unlikely, since a too large fraction tends to destabilize it.

C. $\{N,\Lambda,\Xi\}$ systems

A further difference between the present work and that of Ref. [12] is that here we can also include the Ξ (and Σ) as part of the medium. To investigate the influence of including Ξ's, we perform calculations for a system consisting of N,Λ, and Ξ. The Σ's are excluded since they can easily be annihilated, as stated before. Another motivation for their exclusion is that the Q values for the strong transitions $\Sigma N\to\Lambda N$, $\Sigma\Sigma\to\Lambda\Lambda$, $\Sigma\Lambda\to\Xi N$, and $\Sigma\Xi\to\Lambda\Xi$ are about 78, 156, 50, and 80 MeV, respectively. To Pauli block these processes, we need a rather high density of Λ. On the other hand, the Q value of $\Xi N\to\Lambda\Lambda$ is only about 28 MeV. The presence of Ξ could then help prevent the collapse of the
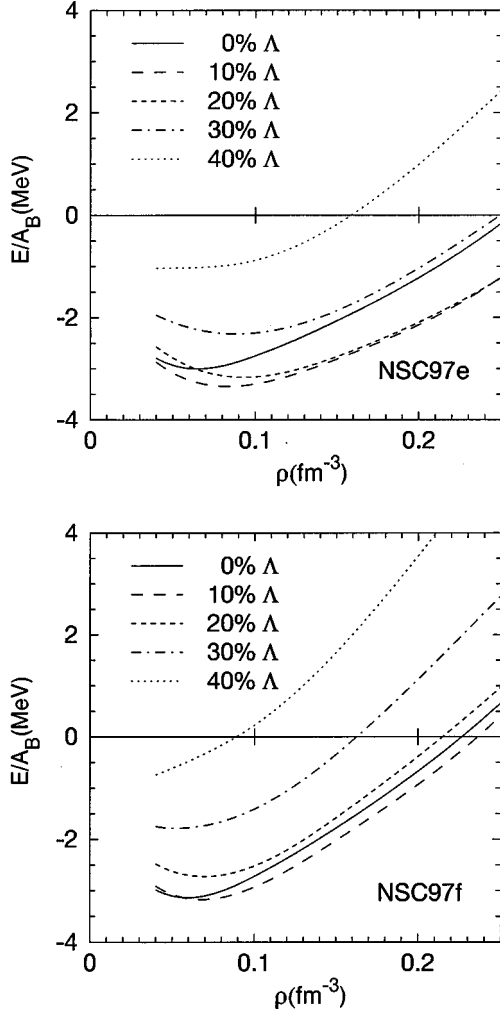
FIG. 4. Saturation of charge-neutral $\{N,\Lambda,\Xi\}$ systems for various fractions $\rho_\Lambda/(\rho_N+\rho_\Lambda+\rho_\Xi)$.

FIG. 5. f_s dependence of the $\{N,\Lambda,\Xi\}$ system for three given fractions of nucleons χ_N.

$\{N,\Lambda,\Xi\}$ system since the $\Lambda\Lambda\to\Xi N$ reaction can be Pauli blocked. The importance of including Ξ's was first pointed out in Ref. [9].

It is interesting to first investigate the charge-neutral systems consisting of only N,Λ, and Ξ. They can be formed with a density distribution of $\rho_p=\rho_n=\rho_{\Xi^0}=\rho_{\Xi^-}$. Our results are shown in Fig. 4. We see that the systems are only loosely bound. The Λ density is too low to Pauli block the $\Xi N\to\Lambda\Lambda$ process. This suggests that a charge-neutral strangeness-rich system is unlikely to be seen in nature or to be created in relativistic heavy-ion collisions.

We now turn to investigating the dependence of the binding energy of the N,Λ,Ξ system on the strangeness per baryon. As discussed in previous works [9–11], this dependence is most relevant to the investigation of relativistic heavy-ion collisions. For this purpose, it is useful to define the fractions $\chi_i=\rho_i/\rho$ for the different species $i=N,\Lambda,\Xi$, as in Eq. (1). The strangeness per baryon for the $\{N,\Lambda,\Xi\}$ systems can then easily be calculated as $f_s=\chi_\Lambda+2\chi_\Xi$. Since we work on the isospin basis, we will only consider systems with $\rho_n=\rho_p=\frac{1}{2}\rho_N$ and $\rho_{\Xi^0}=\rho_{\Xi^-}=\frac{1}{2}\rho_\Xi$. The charge per baryon is then $f_q=\frac{1}{2}(\chi_N-\chi_\Xi)$. For each $\{N,\Lambda,\Xi\}$ system
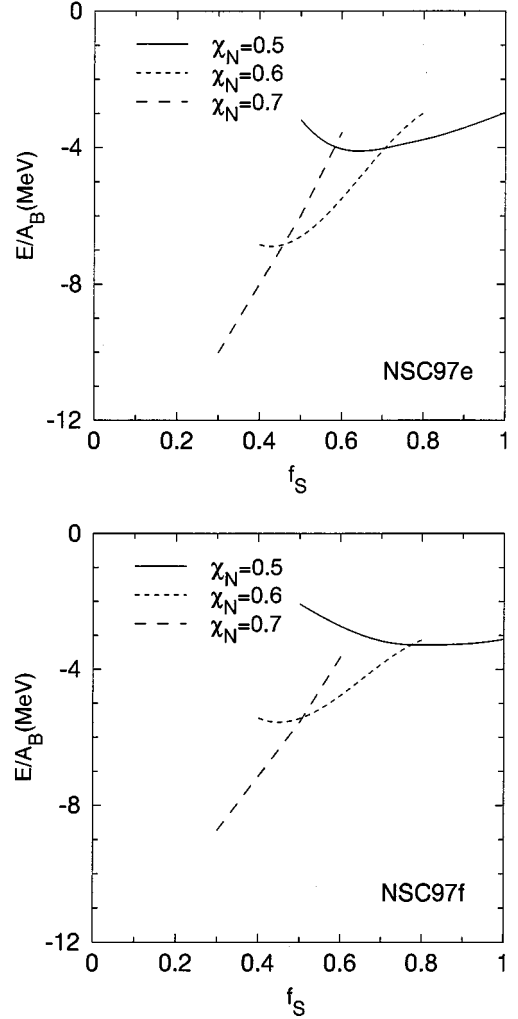
with a given χ_N we carried out calculations for various combinations of $(\chi_\Lambda+\chi_\Xi)=(1-\chi_N)$. In general, we find that the system is less bound for high χ_Ξ, as could already be inferred from comparing Figs. 3 and 4. The reason is that $U_\Xi^{(\Xi)}$ becomes more negative (attractive) as χ_Ξ increases, but this is compensated by positive (repulsive) contributions from $U_{N,\Lambda}^{(\Xi)}$ and $U_\Xi^{(N,\Lambda)}$. The cancellations are large enough to prevent ρ_Ξ from becoming too large, and so the large binding energies as found close to the saturation point of the pure Ξ system (see Fig. 2) cannot be reached.

These calculations allow us to examine the $f_s(f_q)$ dependence of the binding energies at the saturation point of an $\{N,\Lambda,\Xi\}$ system. The results are shown in Fig. 5. In each case, the curves cover the allowed f_s values that can be reached. We see that as f_s (and f_q) increases, the system becomes less bound. When $\chi_N=0.7$, the purely $\{N,\Lambda\}$ system (i.e., $\chi_\Xi=0$) has the lowest binding, but when χ_N gets smaller than 0.6, systems with increasing χ_Ξ are preferred. This follows from the fact that in those cases the curves show a (shallow) minimum. However, when $\chi_N\lesssim0.4$ the system becomes unbound. Our results contradict the results from the relativistic mean-field calculations of Refs. [9–11]
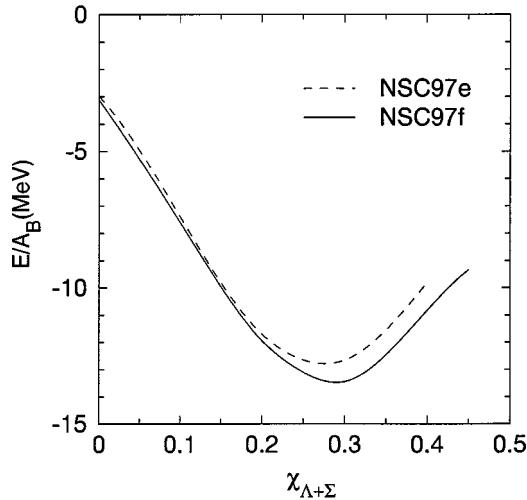
FIG. 6. Saturation of charge neutral $\{N,\Lambda,\Sigma,\Xi\}$ system with $\chi_N = \chi_\Xi$ and $\chi_\Lambda = \chi_\Sigma$, as a function of $\chi_{\Lambda+\Sigma}$.

FIG. 7. f_s dependence of the $\{N,\Lambda,\Sigma,\Xi\}$ system with $\chi_\Lambda = \chi_\Sigma = \chi_\Xi$.

(see Figs. 2 and 3 of Ref. [9]). The differences, of course, could be due to finite-size effects, since these authors consider a shell model for finite $\{N,\Lambda,\Xi\}$ systems (up to very large $A_N = 310$). But it is more likely that the difference is due to the differences in dynamical content of the calculations. This can be understood by observing that the mean-field calculation within the Brueckner-Hartree-Fock approach amounts to neglecting the residual baryon-baryon interaction terms in calculating E/A_B. Moreover, these mean-field results [9] use quite different potentials and include certain rearrangement terms proportional to the actual meson fields.

D. Inclusion of Σ

Although the Σ particles can be easily annihilated, as stated before, their presence largely increases the binding of the system, which might be of relevance in the formation and stability of such a system. To demonstrate the effect of adding Σ's we first consider a charge-neutral $\{N,\Lambda,\Xi\}$ system with $\chi_N = \chi_\Xi$, and so $f_s = 1$. For each choice of $\chi_N = \chi_\Xi$ we can add different fractions of Σ's as long as $(\chi_\Lambda + \chi_\Sigma) = (1 - \chi_N - \chi_\Xi)$. Note that these systems all still have $f_s = 1$. In order to prevent having to show numerous figures or tables, we will here only consider the systems with $\chi_\Lambda = \chi_\Sigma$. The results are shown in Fig. 6. They should be compared with the saturation minima in Fig. 4. We clearly see that adding also Σ's drastically improves the binding of the system compared to adding only Λ's.

The increase in binding due to adding Σ's allows us to further explore the f_s dependence in the region beyond $f_s < 1$. Again, numerous choices for the different particle fractions are possible, but here we will only restrict ourselves to systems with equal fractions for the strange particles, i.e., $\chi_Y \equiv \chi_\Lambda = \chi_\Sigma = \chi_\Xi$. We find that these systems are bound for any value of χ_Y. The f_s dependence of this mixed system is shown in Fig. 7. We see that as f_s increases, the system becomes more bound, except in the low f_s region. Note that at the highest $f_s = 2$, the system is the pure Ξ system as in
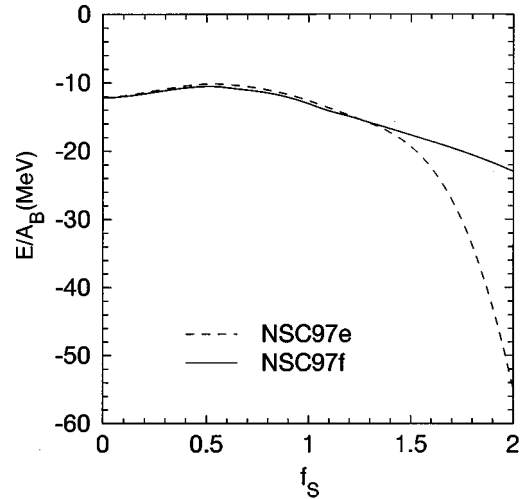
Fig. 2. Of course, our special choice for χ_Y means that the strangeness per baryon can only go up to $f_s = 4/3$, and so the result for $f_s > 4/3$ in Fig. 7 is not calculated, but is rather obtained by simply extrapolating to the pure Ξ result which has $f_s = 2$. Comparing with the results of Fig. 5 for the $\{N,\Lambda,\Xi\}$ system, it is clear that the addition of the Σ component drastically changes the f_s dependence, but it is important to remember here that the system containing Σ is highly unstable against strong decays, as discussed above. The results shown in Fig. 7 perhaps cannot be verified in relativistic heavy-ion collisions. However, it could represent the situation in the core of neutron stars in which the presence of high density e^- can produce a lot of Σ^-, initiated by the reaction $e^- + n \rightarrow \Sigma^- + \nu$.

V. CONCLUSION

We have investigated strange hadron matter in the context of a baryon-baryon potential model based on SU(3) symmetry. The parameters of the potential model were fitted to the NN and YN scattering data, and the assumption of (broken) SU(3) symmetry allows us to extend the model to also describe the other interaction channels that are allowed for the baryon octet; i.e., the $YY, \Xi N, \Xi Y$, and $\Xi\Xi$ interactions. The potential for these interactions is defined without the necessity of having to introduce new free parameters.

The calculations have been carried out by using the Brueckner-Hartree-Fock approximation. Within the framework that we use to define the potential model for the baryon-baryon interactions, we find that the pure Λ system is unbound, whereas the pure Ξ system is more strongly bound and saturates at higher densities than the pure N system. Adding Λ's to pure nuclear matter slightly increases binding, as long as the Λ fraction is less than about 10%. Larger fractions cause a decrease in binding. Adding Ξ's, of importance due to the reaction $\Lambda\Lambda \rightarrow \Xi N$, drastically reduces binding, and so $\{N,\Lambda,\Xi\}$ systems are only (weakly) bound for nucleon fractions larger than 40%. Our results represent a step forward, since the previous Brueckner-Hartree-Fock cal-

culation [12] did not include the Ξ's.

By carrying out extensive calculations for the $\{N,\Lambda,\Xi\}$ and $\{N,\Lambda,\Sigma,\Xi\}$ systems, we have predicted the dependence of the binding energy on the strangeness per baryon, a quantity that is needed to be determined as precisely as possible for identifying the strange quark matter created in relativistic heavy-ion collisions. Our results are significantly different from previous calculations based on relativistic mean-field models. We argue that the differences are mainly due to the two-body correlations, which are neglected in relativistic mean-field models.

To close, we would like to point out that the present work is merely a first step towards a rigorous many-body calculation. In the future, we need to investigate the three-body terms in the Brueckner-Hartree-Fock approach. This is par-ticularly important if one is to give more precise predictions in the higher-density regions. Another reason is that perhaps it is only at that order that the issue of using the gap choice or the continuous choice for the single-particle energies in solving the self-consistent Eqs. (2) and (4) becomes irrel-evant, as was shown in a recent work on ordinary nuclear matter [27]. Our investigation in this direction will be pub-lished elsewhere.

[1] As reviewed by B. Shiva Kumar, Nucl. Phys. **A590**, 29c (1995).

[2] As reviewed by G. Baym, Nucl. Phys. **A590**, 233c (1995); M. Prakash and J.M. Lattimer, *ibid.* **A639**, 433c (1998), and references therein.

[3] A.R. Bodmer, Phys. Rev. D **4**, 1601 (1971).

[4] S.A. Chin and A.K. Kerman, Phys. Rev. Lett. **43**, 1292 (1979); E.P. Gilson and R.L. Jaffe, *ibid.* **71**, 332 (1993).

[5] E. Witten, Phys. Rev. D **30**, 272 (1984).

[6] E. Farhi and R.L. Jaffe, Phys. Rev. D **30**, 2379 (1984); **32**, 2452 (1985).

[7] J. Schaffner-Bielich, C. Greiner, A. Diener, and H. Stöcker, Phys. Rev. C **55**, 3038 (1997).

[8] V.R. Pandharipande, Nucl. Phys. **A178**, 123 (1971).

[9] J. Schaffner, C.B. Dover, A. Gal, C. Greiner, and H. Stöcker, Phys. Rev. Lett. **71**, 1328 (1993).

[10] J. Schaffner, C.B. Dover, A. Gal, D.J. Millener, C. Greiner, and H. Stöcker, Ann. Phys. (N.Y.) **235**, 35 (1994).

[11] A. Gal and C.B. Dover, Nucl. Phys. **A585**, 1c (1995).

[12] H.-J. Schulze, M. Baldo, U. Lombardo, J. Cugnon, and A. Lejeune, Phys. Rev. C **57**, 704 (1998).

[13] C. Greiner, P. Koch, and H. Stöcker, Phys. Rev. Lett. **58**, 1825 (1987).

[14] C. Greiner, D.-H. Rischke, H. Stöcker, and P. Koch, Phys. Rev. D **38**, 2797 (1988).

[15] C. Greiner and H. Stöcker, Phys. Rev. D **44**, 3517 (1991).

[16] H.J. Crawford, M.S. Desai, and G.L. Shaw, Phys. Rev. D **45**, 857 (1992).

[17] A.J. Baltz, C.B. Dover, S.H. Kahana, Y. Pang, T.J. Schlagel, and E. Schnedermann, Phys. Lett. B **325**, 7 (1994).

[18] P.M.M. Maessen, Th.A. Rijken, and J.J. de Swart, Phys. Rev. C **40**, 2226 (1989).

[19] Th.A. Rijken, V.G.J. Stoks, and Y. Yamamoto, Phys. Rev. C **59**, 21 (1999).

[20] V.G.J. Stoks and Th.A. Rijken, Phys. Rev. C **59**, 3009 (1999).

[21] K.A. Brueckner and J.L. Gammel, Phys. Rev. **109**, 1023 (1958).

[22] R. Brockmann and R. Machleidt, Phys. Rev. C **42**, 1965 (1990).

[23] J.-P. Jeukenne, A. Lejeune, and C. Mahaux, Phys. Rep., Phys. Lett. **25C**, 83 (1976).

[24] M. Baldo, I. Bombaci, L.S. Ferreira, G. Giansiracusa, and U. Lombardo, Phys. Rev. C **43**, 2605 (1991); H.Q. Song, M. Baldo, G. Giansiracusa, and U. Lombardo, Phys. Lett. B **411**, 237 (1997).

[25] H.-J. Schulze, J. Cugnon, A. Lejeune, M. Baldo, and U. Lombardo, Phys. Rev. C **52**, 2785 (1995).

[26] M. Lacombe, B. Loiseau, J.M. Richard, R. Vinh Mau, J. Côté, P. Pirés, and R. de Tourreil, Phys. Rev. C **21**, 861 (1980).

[27] H.Q. Song, M. Baldo, G. Giansiracusa, and U. Lombardo, Phys. Rev. Lett. **81**, 1584 (1998).